



Geometric Methods in Dynamics

– *Exercises* –

Sina Ober-Blöbaum, Martin Arnold,

Kathrin Flaschkamp, Dominik Kern

5th - 9th September 2016, Leipzig

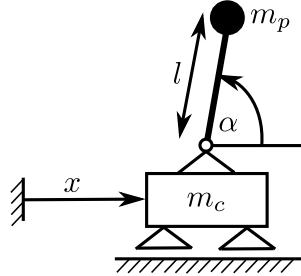
This notebook contains four exercises to supplement the lectures of SAMM2016. All exercises are model problems in order to demonstrate variational integrators (VI) for mechanical and electrical systems with/out holonomic constraints, potentially non-smooth, VI-based optimal control and a Lie-group integrator for ordinary differential equations on manifolds.

Contents

| | |
|--|-----------|
| 1 Simulation of a Pendulum on a Cart by a Variational Integrator | 3 |
| 2 VI-based Optimal Control of a Pendulum on a Cart | 7 |
| 3 Generalized-α Lie Group Time Integration of a Heavy Top | 9 |
| 4 Simulation of an Electric Circuit (LCR) by a VI | 15 |
| 5 Further reading | 20 |

“Exercise! Watching fitness videos will not make you stronger.”

1 Simulation of a Pendulum on a Cart by a Variational Integrator



A pendulum on a cart is to be simulated in the time $t_b \leq t \leq t_e$. The pendulum angle $\alpha(t)$ and the cart position $x(t)$ are chosen as generalized coordinates. Their initial values are $\alpha(0) = -\frac{\pi}{2}$ RAD, $\dot{\alpha}(0) = 0$ RADs $^{-1}$, $x(0) = 0$ m, $\dot{x}(0) = 0$ m $^{-1}$.

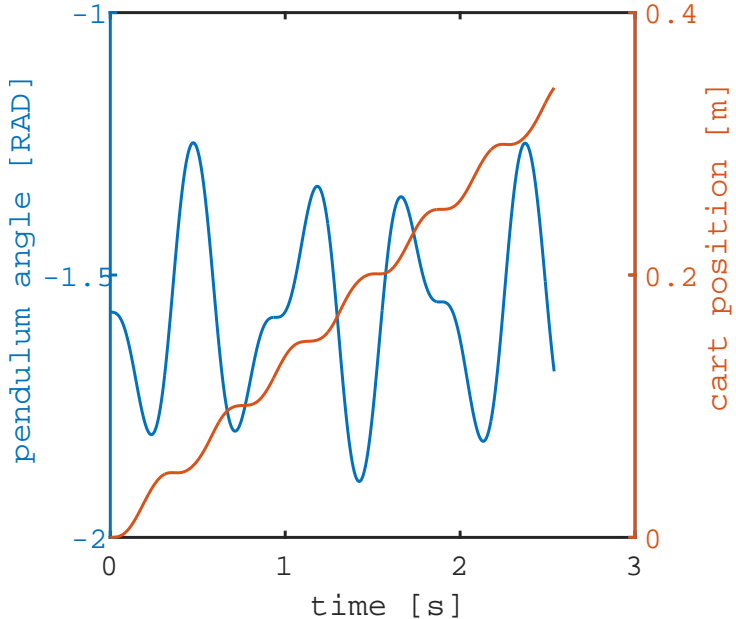
1. implement a variational integrator [3,4], if the cart force $f_c(t) = \hat{f} \sin(2\pi t/T)$ is applied, in oder to obtain $\alpha(t)$ and $x(t)$.
2. implement a variational integrator [3,4], if the cart displacement is prescribed by $x_c(t) = \hat{x} \sin(2\pi t/T)$ (holonomic-rheonomic constraint), in order to obtain $\alpha(t)$ and the Lagrangian multiplier $\lambda(t)$, i.e. the constraint force.

The needed expressions (constraint enforcement on position-level only) are given in the formulary at the end of this section and also template files (octave) are prepared.

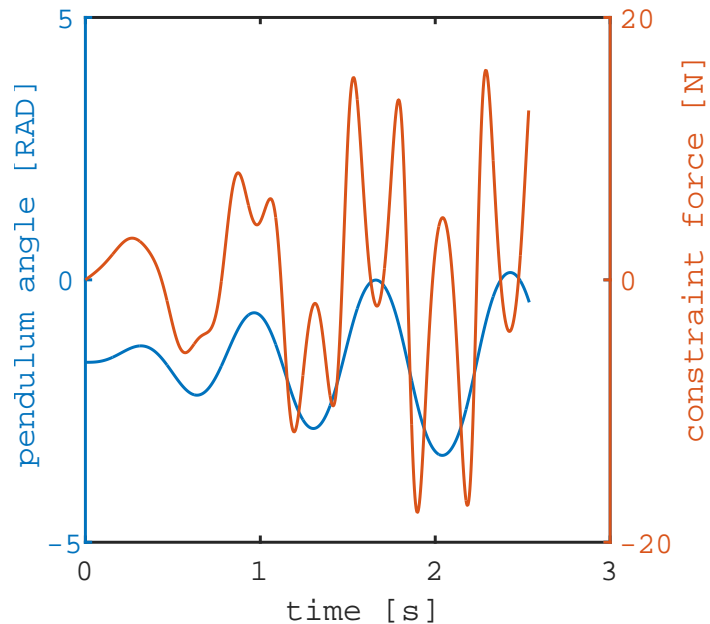
| | | | |
|------------------------------|----------|------------|--|
| m_p | 1 | kg | mass of pendulum |
| m_c | 0.5 | kg | mass of cart |
| l | 0.1 | m | length of pendulum |
| g | 9.81 | ms $^{-2}$ | gravitational acceleration |
| $\hat{f} = \frac{1}{5}m_p g$ | 1.962 | N | forcing coefficient |
| $\hat{x} = \frac{1}{5}l$ | 0.02 | m | displacement coefficient |
| $T = 2\pi\sqrt{l/g}$ | 0.6344 | s | period of forcing/rheonomic constraint |
| t_b | 0 | s | begin time |
| $t_e = 4T$ | 2.5375 | s | end time |
| $h = T/100$ | 0.006344 | s | time step |

verification results

1) forced: $\alpha(t_e) = -1.683545 \text{ RAD}$ $x(t_e) = 0.342659 \text{ m}$



2) constrained: $\alpha(t_e) = -0.429302 \text{ RAD}$ $\lambda(t_e - h) = 12.911663 \text{ N}$



Formulary

| | |
|--|---|
| D'Alembert principle | $0 = \delta \int_{t_k}^{t_{k+1}} L(\mathbf{q}, \dot{\mathbf{q}}) dt + \int_{t_k}^{t_{k+1}} \mathbf{f}(\mathbf{q}, \dot{\mathbf{q}}, t) \cdot \delta \mathbf{q}(t) dt$ |
| Table 1: energy expressions with kinetic energy | $m = m_c + m_p, \quad J = m_p l^2 \quad \text{and} \quad \mathbf{q} = [\alpha, x]^T;$ $T(\mathbf{q}, \dot{\mathbf{q}}) = \frac{1}{2} J \dot{\alpha}^2 - m_p l \dot{\alpha} \dot{x} \sin \alpha + \frac{1}{2} m \dot{x}^2$ $T(\mathbf{q}, \mathbf{p}) = \frac{m p_\alpha^2 + 2 m_p l p_\alpha p_x \sin \alpha + J p_x^2}{2(Jm - m_p^2 l^2 \sin^2 \alpha)}$ |
| potential energy | $V(\mathbf{q}) = m_p g l \sin \alpha$ |
| virtual work of external force on cart | $\delta W^{nc} = f_c(t) \delta x$ |
| rheonomic constraint on cart | $\phi = x(t) - x_c(t) = 0$ |

Table 2: discretization by linear approximation and mid-point rule for one time step

$$\begin{aligned}
h &= t_{k+1} - t_k \\
\mathbf{q}_d(t) &= \mathbf{q}_k + (\mathbf{q}_{k+1} - \mathbf{q}_k) \frac{t-t_k}{h} \quad \text{for} \quad t_k \leq t < t_{k+1} \\
L_k &= L_d(\mathbf{q}_k, \mathbf{q}_{k+1}) = h L\left(\mathbf{q}_d(t_k + h/2), \dot{\mathbf{q}}_d(t_k + h/2)\right) = h L\left(\frac{\mathbf{q}_{k+1} + \mathbf{q}_k}{2}, \frac{\mathbf{q}_{k+1} - \mathbf{q}_k}{h}\right) \\
\mathbf{f}_k^- &= \mathbf{f}_d^-(\mathbf{q}_k, \mathbf{q}_{k+1}, t_k, t_{k+1}) = \frac{h}{2} \mathbf{f}\left(\frac{\mathbf{q}_{k+1} + \mathbf{q}_k}{2}, \frac{\mathbf{q}_{k+1} - \mathbf{q}_k}{h}, \frac{t_{k+1} + t_k}{2}\right) \\
\mathbf{f}_k^+ &= \mathbf{f}_d^+(\mathbf{q}_k, \mathbf{q}_{k+1}, t_k, t_{k+1}) = \mathbf{f}_k^- \\
\phi(\mathbf{q}_k) &= \mathbf{0}
\end{aligned}$$

Table 3: position-momentum-form

$$\begin{aligned}
\mathbf{p}_k &= -D_1 L_d(\mathbf{q}_k, \mathbf{q}_{k+1}) - \mathbf{f}_d^-(\mathbf{q}_k, \mathbf{q}_{k+1}, t_k, t_{k+1}) + \lambda_k h D\phi(\mathbf{q}_k) &= -D_1 L_k - \mathbf{f}_k^- + \lambda_k h D\phi_k \\
\mathbf{p}_{k+1} &= D_2 L_d(\mathbf{q}_k, \mathbf{q}_{k+1}) + \mathbf{f}_d^+(\mathbf{q}_k, \mathbf{q}_{k+1}, t_k, t_{k+1}) &= D_2 L_k + \mathbf{f}_k^+
\end{aligned}$$

Table 4: mass matrix for conversion between velocities and momenta (post-processing)

$$\mathbf{M} = \begin{bmatrix} J & -m_p l \sin \alpha \\ \text{sym.} & m \end{bmatrix} \quad \mathbf{p} = \mathbf{M} \dot{\mathbf{q}} \quad \dot{\mathbf{q}} = \mathbf{M}^{-1} \mathbf{p}$$

Table 5: iteration equation in order to obtain \mathbf{q}_{k+1} (and if constrained λ_k)

$$\begin{aligned} 0 &= \mathbf{p}_k + D_1 L_k + \mathbf{f}_k^- \quad (-\lambda_k h D\phi_k) \\ (0) &= \phi(\mathbf{q}_{k+1}) \end{aligned}$$

Table 6: update equation in order to obtain \mathbf{p}_{k+1} (ignoring constraint on velocity level)

$$\mathbf{p}_{k+1} = D_2 L_k + \mathbf{f}_k^+$$

Table 7: expressions for iteration-, update-equation and for tangent (Newton-solver)

$$\Delta\alpha = \alpha_{k+1} - \alpha_k, \quad \Sigma\alpha = \alpha_{k+1} + \alpha_k, \quad \Delta x = x_{k+1} - x_k, \quad \Sigma x = x_{k+1} + x_k$$

$$\begin{aligned} D_1 L_k &= \frac{1}{h} \begin{bmatrix} m_p l \Delta x (\sin \frac{\Sigma\alpha}{2} - \frac{\Delta\alpha}{2} \cos \frac{\Sigma\alpha}{2}) - J \Delta\alpha - \frac{h^2}{2} m_p g l \cos \frac{\Sigma\alpha}{2} \\ -m \Delta x + m_p l \Delta\alpha \sin \frac{\Sigma\alpha}{2} \end{bmatrix} \\ D_2 L_k &= \frac{1}{h} \begin{bmatrix} -m_p l \Delta x (\sin \frac{\Sigma\alpha}{2} + \frac{\Delta\alpha}{2} \cos \frac{\Sigma\alpha}{2}) + J \Delta\alpha - \frac{h^2}{2} m_p g l \cos \frac{\Sigma\alpha}{2} \\ m \Delta x - m_p l \Delta\alpha \sin \frac{\Sigma\alpha}{2} \end{bmatrix} \\ \mathbf{f}_k^- &= \mathbf{f}_k^+ = \frac{h}{2} \begin{bmatrix} 0 \\ f_c(t_k + h/2) \end{bmatrix} \\ D\phi_k &= \begin{bmatrix} 0 \\ 1 \end{bmatrix} \\ D_2 D_1 L_k &= \frac{1}{h} \begin{bmatrix} \frac{1}{4} m_p l \Delta\alpha \Delta x \sin \frac{\Sigma\alpha}{2} - J + \frac{h^2}{4} m_p g l \sin \frac{\Sigma\alpha}{2} & m_p l (\sin \frac{\Sigma\alpha}{2} - \frac{\Delta\alpha}{2} \cos \frac{\Sigma\alpha}{2}) \\ m_p l (\sin \frac{\Sigma\alpha}{2} + \frac{\Delta\alpha}{2} \cos \frac{\Sigma\alpha}{2}) & -m \end{bmatrix} \\ D_2 \mathbf{f}_k^- &= \begin{bmatrix} 0 \\ 0 \end{bmatrix} \end{aligned}$$

2 VI-based Optimal Control of a Pendulum on a Cart

1. Consider an optimal control problem

$$\begin{aligned} \min & \int_0^T C(x(t), u(t)) dt + \Phi(x(T)) \\ \text{s.t. } & \dot{x}(t) = f(x(t), u(t)), x(0) = x^0, 0 = \Psi(x(T)) \end{aligned}$$

- Show that for fixed final time T , the Hamiltonian of the optimal control problem along an optimal solution is constant for all $t \in [0, T]$. (We assume that the optimal control is differentiable.)

Hint: Proof that $\frac{d}{dt} H = 0$ and make use of the fact that the optimal control problem does not depend on time explicitly, so $\frac{\partial H}{\partial t} = 0$.

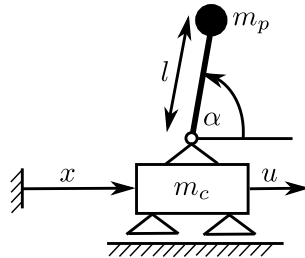


Figure 1: Pendulum on cart, assume control force applied to cart

2. Return to the example of the cart-pendulum with force control. Our aim is to compute an energy minimal swing-up, i.e. a control trajectory that steers the system from the downward rest position $((x^0, \alpha^0, \dot{x}^0, \dot{\alpha}^0) = (0, -\frac{\pi}{2}, 0, 0))$ to the upward rest position $((x^T, \alpha^T, \dot{x}^T, \dot{\alpha}^T) = (0, \frac{\pi}{2}, 0, 0))$ with minimal control effort,

$$J(u) = \int_0^T \frac{1}{2} u^2(t) dt.$$

- Use yesterday's code for simulating the cart-pendulum to try and manually design any control function that swings up the pendulum. (If you give up after a few trials thinking there must be a better way, that's good!)
- Write a program that solves the optimal control problem by a direct method with full discretization by discrete Euler-Lagrange equations [6] and Octave's sqp-solver. Compute an optimal swing-up for final time $T = 0.5 s$ and a step size $h = 0.05$.

Hints:

- Define a vector of optimization variables that contains discrete states and discrete controls. It might be helpful to use the *reshape* command to split up this vector back into q_d , u_d inside functions (cf. template).
- Define an initial value of correct size (need not be a feasible point!).
- Provide a function for the discrete cost function, e.g.

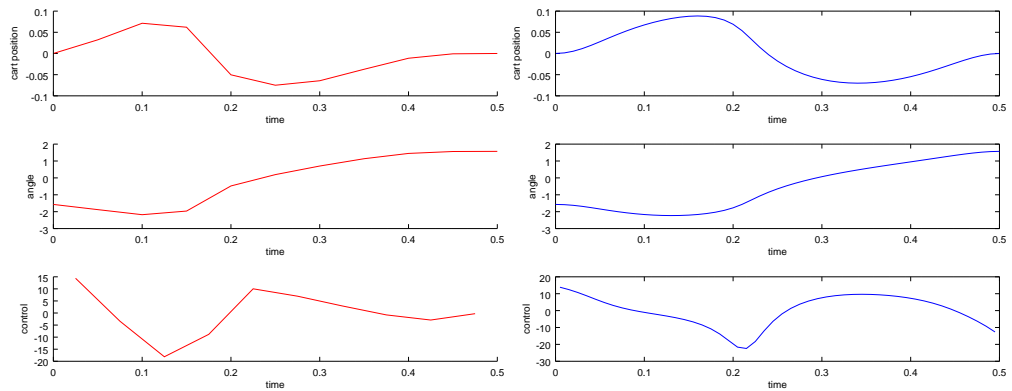
$$J_d(u_d) = \sum_{i=1}^N 0.5 \cdot h \cdot u_i^2.$$

- Provide a function for the equality constraints, where boundary conditions and discrete Euler-Lagrange equations go in. Reuse the $D_1 L_d$, $D_2 L_d$ functions from yesterday.
- Box constraints often help the sqp-solver to converge. Here, try

$$x_k \in [-0.2, 0.2], \quad \alpha_k \in [-\pi, \pi], \quad u_k \in [-50, 50] \quad \text{for } k = 0, 1, 2, \dots$$

- Use Octave's sqp-function as was described in *main_getting_startet.m* or see "help sqp".
- You can get solutions with finer discretizations ($N = 20, 30, 40, 50$) more easily if you interpolate previously computed solutions to use them as initial guesses.
- What would be important changes in code when switching back to a standard explicit Euler (or higher order Runge-Kutta) discretization?
- How would you modify/extend/improve your code to solve other optimal control problems in future?

Verification: Swing-up solution for discretizations with step-size $h = 0.05$ (left) and $h = 0.01$ (right).



3 Generalized- α Lie Group Time Integration of a Heavy Top

Lie group and Lie algebra

The tilde operator $(\tilde{\bullet}) : \mathbb{R}^3 \rightarrow \mathfrak{so}(3)$ maps vectors $\Omega \in \mathbb{R}^3$ to

$$\tilde{\Omega} := \begin{pmatrix} 0 & -\Omega_3 & \Omega_2 \\ \Omega_3 & 0 & -\Omega_1 \\ -\Omega_2 & \Omega_1 & 0 \end{pmatrix} \in \mathfrak{so}(3) = \{ \mathbf{A} \in \mathbb{R}^{3 \times 3} : \mathbf{A} + \mathbf{A}^\top = \mathbf{0} \}.$$

The corresponding matrix exponential

$$\exp_{SO(3)}(\tilde{\Omega}) = \sum_{i=0}^{\infty} \frac{1}{i!} \tilde{\Omega}^i$$

is a mapping from Lie algebra $\mathfrak{g} := \mathfrak{so}(3)$ to Lie group

$$G := SO(3) = \{ \mathbf{R} \in \mathbb{R}^{3 \times 3} : \mathbf{R}\mathbf{R}^\top = \mathbf{I}_3, \det \mathbf{R} = +1 \}.$$

It may be evaluated efficiently by Rodrigues' formula

$$\exp_{SO(3)}(\tilde{\Omega}) = \mathbf{I}_3 + \frac{\sin \Phi}{\Phi} \tilde{\Omega} + \frac{1 - \cos \Phi}{\Phi^2} \tilde{\Omega}^2 \quad \text{with } \Phi := \|\Omega\|_2.$$

Exercises

- a) Verify Rodrigues' formula comparing the series expansions of \exp , \sin and \cos :

$$\exp z = \sum_{k=0}^{\infty} \frac{z^k}{k!}, \quad \sin z = \sum_{k=0}^{\infty} (-1)^k \frac{z^{2k+1}}{(2k+1)!}, \quad \cos z = \sum_{k=0}^{\infty} (-1)^k \frac{z^{2k}}{(2k)!}.$$

Hint: The Cayley-Hamilton theorem implies

$$\tilde{\Omega}^3 + a_2 \tilde{\Omega}^2 + a_1 \tilde{\Omega} + a_0 \mathbf{I}_3 = \mathbf{0}$$

with $a_0, a_1, a_2 \in \mathbb{R}$ denoting the coefficients of the characteristic polynomial

$$\chi_\mu(\tilde{\Omega}) = \det(\mu \mathbf{I}_3 - \tilde{\Omega}) = \mu^3 + a_2 \mu^2 + a_1 \mu + a_0.$$

Use this identity to express $\tilde{\Omega}^{2k+1}$, ($k \geq 1$), and $\tilde{\Omega}^{2k}$, ($k \geq 2$), in terms of \mathbf{I}_3 , $\tilde{\Omega}$ and $\tilde{\Omega}^2$.

b) Use `octave` to verify numerically $\mathbf{R}, \mathbf{R}_0 \in \text{SO}(3)$ for matrices

$$\mathbf{R}_0 := \begin{pmatrix} \frac{1}{2} & 0 & -\frac{1}{2}\sqrt{3} \\ 0 & 1 & 0 \\ \frac{1}{2}\sqrt{3} & 0 & \frac{1}{2} \end{pmatrix} \quad \text{and} \quad \mathbf{R} := \mathbf{R}_0 \exp(\tilde{\boldsymbol{\Omega}}) \quad \text{with} \quad \boldsymbol{\Omega} = \begin{pmatrix} 3 \\ -1 \\ 8 \end{pmatrix},$$

i.e., check that the residuals

$$\|\mathbf{R}_0 \mathbf{R}_0^\top - \mathbf{I}_3\|_2, \quad \det \mathbf{R}_0 - 1, \quad \|\mathbf{R} \mathbf{R}^\top - \mathbf{I}_3\|_2, \quad \det \mathbf{R} - 1$$

remain in the size of round-off errors. Repeat this numerical experiment for other vectors $\boldsymbol{\Omega} \in \mathbb{R}^3$.

Spinning top in Lie group formulation: The ODE case



Figure Spinning top with its tip being fixed to the origin, see O. Brüls, A. Cardona: *On the use of Lie group time integrators in multibody dynamics*. J. Comput. Nonlinear Dynam. **5**, 031002 (2010).

The figure shows a frequently used benchmark problem in Lie group time integration: A spinning heavy top that has its tip being fixed to the origin and moves under the influence of gravity [2]. The top has three rotational degrees of freedom with a rotation matrix $\mathbf{R}(t) \in \text{SO}(3)$ describing its orientation. In the Lie group setting, the equilibrium conditions are written in the general form

$$\mathbf{M}(q)\dot{\mathbf{v}} = \mathbf{f}(q, \mathbf{v})$$

with mass matrix \mathbf{M} , force vector \mathbf{f} , position coordinates $q = \mathbf{R} \in \text{SO}(3)$ and velocity coordinates $\mathbf{v} = \boldsymbol{\Omega} \in \mathbb{R}^3$ that are given by the top's angular velocity [1].

Model data

- $[t_0, t_e]$ Time interval of interest $[t_0, t_e] = [0.0\text{s}, 2.0\text{s}]$
 \mathbf{R}_0 Initial configuration, $\mathbf{R}(t_0) = \mathbf{R}_0 = \mathbf{I}_3$
 $\boldsymbol{\Omega}_0$ Initial value of angular velocity, $\boldsymbol{\Omega}(t_0) = \boldsymbol{\Omega}_0 = (0, 1.5, -0.0461538)^\top \text{ rad/s}$
 m Mass of the top, $m = 15.0\text{kg}$
 \mathbf{X} Coordinates of the top's center of gravity, $\mathbf{X} = (0.0\text{m}, 1.0\text{m}, 0.0\text{m})^\top$
 $\bar{\mathbf{J}}$ Inertia tensor w.r.t. the fixed point,
 $\bar{\mathbf{J}} = \text{diag} (15.234375 \text{ kg m}^2, 0.46875 \text{ kg m}^2, 15.234375 \text{ kg m}^2)$
 $\boldsymbol{\gamma}$ Gravity vector, $\boldsymbol{\gamma} = (0.0 \text{ m/s}^2, 0.0 \text{ m/s}^2, -9.81 \text{ m/s}^2)^\top$

Reference solution

The dynamical behaviour of the spinning top is illustrated by the time histories of the angular velocity $\boldsymbol{\Omega}$ and the diagonal entries of \mathbf{R} :

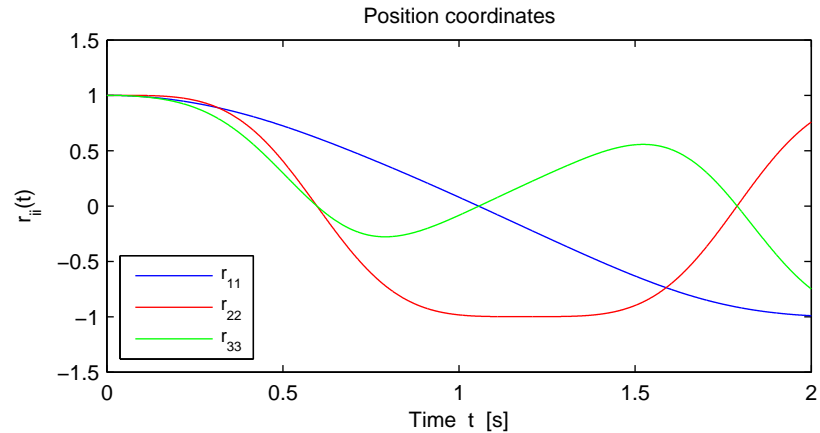


Figure Reference solution for position coordinates.

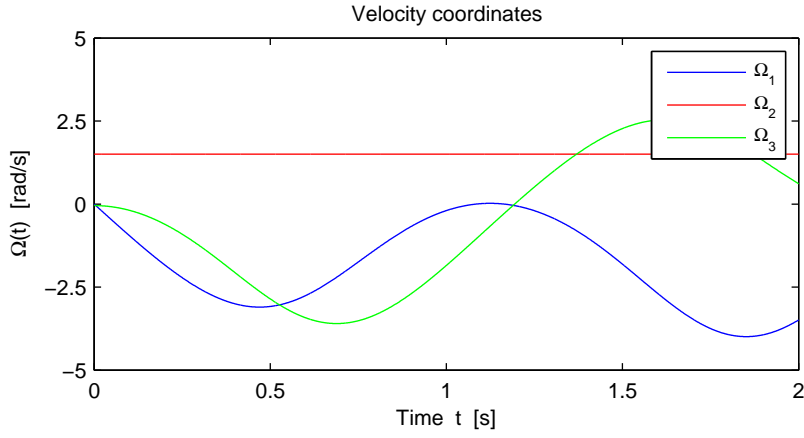


Figure Reference solution for velocity coordinates.

Exercises

- For time integration, the equilibrium conditions $\bar{\mathbf{J}}\dot{\boldsymbol{\Omega}} + \boldsymbol{\Omega} \times \bar{\mathbf{J}}\boldsymbol{\Omega} = \mathbf{X} \times \mathbf{R}^\top m\boldsymbol{\gamma}$ are expressed in the general form $\mathbf{M}(q)\dot{\mathbf{v}} = \mathbf{f}(q, \mathbf{v})$. Write the mass matrix $\mathbf{M}(q)$ and the force vector $\mathbf{f}(q, \mathbf{v})$ in terms of $q = \mathbf{R}$, $\mathbf{v} = \boldsymbol{\Omega}$, $\bar{\mathbf{J}}$, \mathbf{X} , m and $\boldsymbol{\gamma}$.
- In generalized- α time integration, the starting values q_0 and \mathbf{v}_0 are defined by the initial values \mathbf{R}_0 and $\boldsymbol{\Omega}_0$. Write an `octave` script to compute starting values $\dot{\mathbf{v}}_0$ with

$$\mathbf{M}(q_0)\dot{\mathbf{v}}_0 = \mathbf{f}(q_0, \mathbf{v}_0)$$

and starting values

$$\mathbf{a}_0 = \dot{\mathbf{v}}_0 + \Delta_\alpha h \frac{\dot{\mathbf{v}}_{sh} - \dot{\mathbf{v}}_{-sh}}{2sh}$$

with $s := 0.1$ and vectors $\dot{\mathbf{v}}_{sh}$, $\dot{\mathbf{v}}_{-sh}$ satisfying

$$\mathbf{M}(q_{sh})\dot{\mathbf{v}}_{sh} = \mathbf{f}(q_{sh}, \mathbf{v}_{sh}), \quad \mathbf{M}(q_{-sh})\dot{\mathbf{v}}_{-sh} = \mathbf{f}(q_{-sh}, \mathbf{v}_{-sh})$$

for $q_{\pm sh} = q_0 \circ \exp(\pm sh\tilde{\mathbf{v}}_0 + s^2 h^2 \tilde{\mathbf{v}}_0/2)$, $\mathbf{v}_{\pm sh} = \mathbf{v}_0 \pm sh\dot{\mathbf{v}}_0$.

Here, we denote $\Delta_\alpha := \alpha_m - \alpha_f$ and use algorithmic parameters

$$\alpha_m = \frac{2\rho_\infty - 1}{\rho_\infty + 1}, \quad \alpha_f = \frac{\rho_\infty}{\rho_\infty + 1}, \quad \gamma = \frac{1}{2} + \alpha_f - \alpha_m, \quad \beta = \frac{1}{4}(\gamma + \frac{1}{2})^2$$

with $\rho_\infty \in [0, 1]$ denoting the (given) damping ratio at infinity. Check your `octave` script for parameter values $\rho_\infty = 0.9$, $h = 1.0 \times 10^{-3}$ s and $s = 0.1$ that should result in starting values

$$\dot{\mathbf{v}}_0 = \begin{pmatrix} -9.591976398461540 \text{ rad/s}^2 \\ 0.0000000000000000 \text{ rad/s}^2 \\ 0.0000000000000000 \text{ rad/s}^2 \end{pmatrix}, \quad \mathbf{a}_0 = \begin{pmatrix} -9.591976455653450 \text{ rad/s}^2 \\ 0.0000000000000000 \text{ rad/s}^2 \\ 0.001496519648117 \text{ rad/s}^2 \end{pmatrix}.$$

- c) Write an `octave` script to evaluate for given data ρ_∞ , h , q_n , \mathbf{v}_n , $\dot{\mathbf{v}}_n$, \mathbf{a}_n and $\mathbf{x} := \Delta \mathbf{q}_n$ the residual

$$\mathbf{r}_{n+1}^{(\text{ODE})}(\mathbf{x}) := \mathbf{M}(q_{n+1}(\mathbf{x}))\dot{\mathbf{v}}_{n+1}(\mathbf{x}) - \mathbf{f}(q_{n+1}(\mathbf{x}), \mathbf{v}_{n+1}(\mathbf{x}))$$

in the equilibrium conditions for

$$\begin{aligned} q_{n+1}(\mathbf{x}) &= q_n \circ \exp(h\tilde{\mathbf{x}}), \\ \mathbf{v}_{n+1}(\mathbf{x}) &= \frac{\gamma}{\beta}\mathbf{x} + (1 - \frac{\gamma}{\beta})\mathbf{v}_n + h(1 - \frac{\gamma}{2\beta})\mathbf{a}_n, \\ \dot{\mathbf{v}}_{n+1}(\mathbf{x}) &= \frac{1 - \alpha_m}{\beta(1 - \alpha_f)}\left(\frac{\mathbf{x} - \mathbf{v}_n}{h} - 0.5\mathbf{a}_n\right) + \frac{\mathbf{a}_n - \alpha_f\dot{\mathbf{v}}_n}{1 - \alpha_f} \end{aligned}$$

and algorithmic parameters α_m , α_f , β , γ as defined above. Use this script to solve the nonlinear system

$$\mathbf{0} = \Psi_{n+1,h}^{(\text{ODE})}(\mathbf{x}) := h\mathbf{r}_{n+1}^{(\text{ODE})}(\mathbf{x})$$

for $n = 0$, $h = 1.0 \times 10^{-3}$ s by Newton's method with starting guess

$$\mathbf{x}^{(0)} = \Delta \mathbf{q}_n^{(0)} := \mathbf{v}_n + 0.5h\mathbf{a}_n$$

for obtaining the numerical solution at $t_1 = t_0 + h = h$: $q_1 = q_1(\mathbf{x})$, $\mathbf{v}_1 = \mathbf{v}_1(\mathbf{x})$, $\dot{\mathbf{v}}_1 = \dot{\mathbf{v}}_1(\mathbf{x})$,

$$\mathbf{a}_1 = \mathbf{a}_1(\mathbf{x}) = \frac{1}{\beta h}(\mathbf{x} - \mathbf{v}_0 - (0.5 - \beta)h\mathbf{a}_0).$$

- d) Proceed in time steps $t_n \rightarrow t_{n+1} = t_n + h$ from $t_0 = 0.0$ s to $t_e = 2.0$ s to compute iteratively the numerical solution

$$q_n \approx q(t_n), \quad \mathbf{v}_n \approx \mathbf{v}(t_n), \quad \dot{\mathbf{v}}_n \approx \dot{\mathbf{v}}(t_n), \quad \mathbf{a}_n \approx \dot{\mathbf{v}}(t_n + \Delta_\alpha h)$$

for all $n > 0$ with $t_0 + nh \leq t_e$. Compare your results with the reference solution being shown above.

Spinning top in Lie group formulation: Some DAE aspects

Exercises

- a) Verify that the group operation $(\mathbf{R}_a, \mathbf{x}_a) \circ (\mathbf{R}_b, \mathbf{x}_b) = (\mathbf{R}_a \mathbf{R}_b, \mathbf{x}_a + \mathbf{x}_b)$ in Lie group $G = \text{SO}(3) \times \mathbb{R}^3$ corresponds to the matrix multiplication of block matrices

$$\begin{pmatrix} \mathbf{R} & \mathbf{0}_{3 \times 3} & \mathbf{0}_{3 \times 1} \\ \mathbf{0}_{3 \times 3} & \mathbf{I}_3 & \mathbf{x} \\ \mathbf{0}_{1 \times 3} & \mathbf{0}_{1 \times 3} & 1 \end{pmatrix} \in \mathbb{R}^{7 \times 7}.$$

- b) In the same way, the elements $\tilde{\mathbf{v}}$ of the Lie algebra $\mathfrak{g} = \mathfrak{so}(3) \times \mathbb{R}^3$ may be identified with matrices

$$\begin{pmatrix} \tilde{\boldsymbol{\Omega}} & \mathbf{0}_{3 \times 3} & \mathbf{0}_{3 \times 1} \\ \mathbf{0}_{3 \times 3} & \mathbf{0}_{3 \times 3} & \mathbf{u} \\ \mathbf{0}_{1 \times 3} & \mathbf{0}_{1 \times 3} & 0 \end{pmatrix} \in \mathbb{R}^{7 \times 7}.$$

Here, we split $\mathbf{v} \in \mathbb{R}^6$ according to $\mathbf{v} = (\boldsymbol{\Omega}^\top, \mathbf{u}^\top)^\top$ into its components $\boldsymbol{\Omega}$ (angular velocity in the body fixed frame) and \mathbf{u} (translation velocity in the inertial frame). Use this expression to prove

$$\exp_{\text{SO}(3) \times \mathbb{R}^3}(\tilde{\mathbf{v}}) = \sum_{i=0}^{\infty} \frac{1}{i!} \tilde{\mathbf{v}}^i = \begin{pmatrix} \exp_{\text{SO}(3)}(\tilde{\boldsymbol{\Omega}}) & \mathbf{0}_{3 \times 3} & \mathbf{0}_{3 \times 1} \\ \mathbf{0}_{3 \times 3} & \mathbf{I}_3 & \mathbf{u} \\ \mathbf{0}_{1 \times 3} & \mathbf{0}_{1 \times 3} & 1 \end{pmatrix}.$$

- c) In $\text{SO}(3) \times \mathbb{R}^3$, the equations of motion for the spinning top are given by

$$\begin{aligned} \dot{\mathbf{R}} &= \mathbf{R}\tilde{\boldsymbol{\Omega}}, \\ \dot{\mathbf{x}} &= \mathbf{u}, \\ \mathbf{J}\dot{\boldsymbol{\Omega}} + \boldsymbol{\Omega} \times \mathbf{J}\boldsymbol{\Omega} &= -\mathbf{X} \times \boldsymbol{\lambda}, \\ m\dot{\mathbf{u}} &= m\boldsymbol{\gamma} + \mathbf{R}\boldsymbol{\lambda}, \\ \mathbf{0} &= \mathbf{X} - \mathbf{R}^\top \mathbf{x} \end{aligned}$$

with \mathbf{J} denoting the top's inertia tensor w.r.t. its center of mass, $\mathbf{J} = \bar{\mathbf{J}} + m\tilde{\mathbf{X}}\tilde{\mathbf{X}}$.

Differentiate the holonomic constraint $\mathbf{X} - \mathbf{R}^\top \mathbf{x} = \mathbf{0}$ twice w.r.t. t to get the hidden constraints at velocity level and at acceleration level. Use these hidden constraints to eliminate analytically the Lagrange multipliers $\boldsymbol{\lambda}$ and to show the equivalence to the (unconstrained) equations of motion in $G = \text{SO}(3)$.

4 Simulation of an Electric Circuit (LCR) by a VI

Consider the graph consisting of four boundary edges and two diagonal edges of a square (see Figure 2). On each edge of this graph, we have a triple of capacitor (with capacitance $C_i = 1$, $i = 1, \dots, 6$), inductor (with inductance $L_i = 1$, $i = 1, \dots, 5$) and resistor (with resistance $R_i = 0.001$, $i = 1, \dots, 6$) except on one edge. On this edge, there is only one capacitor and one resistor which leaves a degenerate Lagrangian. The corresponding planar graph consists of $n = 6$ branches and $m + 1 = 4$ nodes, thus we have $l = 3$ meshes.

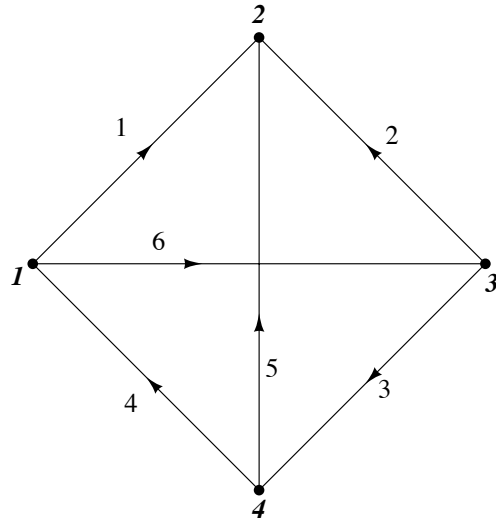


Figure 2: Graph representation of a RLC circuit [5].

- (i) Derive the Kirchhoff Constraint matrix $K \in \mathbb{R}^{n,m}$ and the Fundamental Loop matrix $K_2 \in \mathbb{R}^{n,n-m}$ (with the fourth node assumed to be grounded) and check if $\text{im}(K_2) \perp \text{im}(K)$ is satisfied.
- (ii) Formulate the Lagrange-d'Alembert-Pontryagin principle in the space of branches and the reduced space of meshes and derive the corresponding Euler-Lagrange equations. Is the Lagrangian on the reduced space still singular?
- (iii) Derive the time stepping schemes in mesh space for three variational integrators: the Euler forward variational integrator, the Euler backward variational integrator and the midpoint rule variational integrator.
- (iv) Simulate the circuit behaviour in mesh space formulation with the three variational integrators and a Runge Kutta 4 method (without stepsize control) and compare the results with the exact solution (see template files for the RK integrator and the exact solution). Use the following parameters

- a) integration time $T = 30$, stepsize $h = 0.1$, no resistor $R_i = 0$, $i = 1, \dots, 6$,
- b) integration time $T = 700$ and $T = 2000$, stepsize $h = 0.4$, no resistor,
- c) add on each branch a small resistor with resistance $R_i = 0.001$, $i = 1, \dots, 6$
and simulate the circuit in the reduced space with $T = 700$, stepsize $h = 0.4$.

For each case, use the initial mesh charges $\tilde{q}_i = 1$ and mesh currents $\tilde{v}_i = 0$, $i = 1, 2, 3$. Compare the branch current evolution and the energy behaviour.

Hint for midpoint rule variational integrator:

For the midpoint rule, we introduce internal stages $\tilde{V}_k = \tilde{v}(t_k + \frac{1}{2}h)$, $\tilde{Q}_k = \tilde{q}_k + \frac{1}{2}h\tilde{V}_k$, $\tilde{P}_k = \frac{\partial \mathcal{L}^M}{\partial \tilde{v}}(\tilde{Q}_k, \tilde{V}_k)$ at the midpoints of each time interval. The approximations at the nodes are then determined by the internal stages via $\tilde{q}_{k+1} = \tilde{q}_k + h\tilde{V}_k$ and $\tilde{p}_{k+1} = \tilde{p}_k + h\frac{\partial \mathcal{L}^M}{\partial \tilde{q}}(\tilde{Q}_k, \tilde{V}_k)$. By taking variations $\delta\tilde{q}_k, \delta\tilde{Q}_k, \delta\tilde{p}_k, \delta\tilde{P}_k, \delta\tilde{V}_k$ for the following discrete Lagrange-d'Alembert-Pontryagin principle with $\delta q_N = 0$ but free $\delta\tilde{q}_0$ and initial value \tilde{q}^0

$$\begin{aligned} \delta \left\{ h \sum_{k=0}^{N-1} \left(\mathcal{L}^M(\tilde{Q}_k, \tilde{V}_k) + \left\langle \tilde{P}_k, \frac{\tilde{Q}_k - \tilde{q}_k}{h} - \frac{1}{2}\tilde{V}_k \right\rangle + \left\langle \tilde{p}_{k+1}, \frac{\tilde{q}_{k+1} - \tilde{q}_k}{h} - \tilde{V}_k \right\rangle \right) + \langle \tilde{p}_0, \tilde{q}_0 - \tilde{q}^0 \rangle \right\} \\ + h \sum_{k=0}^{N-1} f_L^M(\tilde{Q}_k, \tilde{V}_k, \tau_k) \delta\tilde{Q}_k = 0 \end{aligned} \quad (1)$$

we obtain an integrator that is equivalent to a Runge-Kutta scheme with coefficients $a = \frac{1}{2}$, $b = 1$, $c = \frac{1}{2}$ (implicit midpoint rule integrator) applied to the corresponding Hamiltonian system.

Verification results

- (iii)
 - Forward Euler variational integration scheme: For given $(\tilde{q}_0, \tilde{v}_0)$, use $\tilde{p}_0 = K_2^T L K_2 \tilde{v}_0$ to compute \tilde{p}_0 . Then, use the iteration scheme

$$\begin{pmatrix} I & 0 & 0 \\ 0 & K_2^T L K_2 & -I \\ hK_2^T C K_2 & hK_2^T R K_2 & I \end{pmatrix} \begin{pmatrix} \tilde{q}_k \\ \tilde{v}_k \\ \tilde{p}_k \end{pmatrix} = \begin{pmatrix} I & hI & 0 \\ 0 & 0 & 0 \\ 0 & 0 & I \end{pmatrix} \begin{pmatrix} \tilde{q}_{k-1} \\ \tilde{v}_{k-1} \\ \tilde{p}_{k-1} \end{pmatrix} \quad \text{for } k = 1, \dots, N \quad (2)$$

to compute $\tilde{q}_1, \dots, \tilde{q}_N$, $\tilde{v}_1, \dots, \tilde{v}_N$ and $\tilde{p}_1, \dots, \tilde{p}_N$.

- Backward Euler variational integration scheme: For given $(\tilde{q}_0, \tilde{v}_0)$ compute \tilde{p}_0 via $\tilde{p}_0 = K_2^T L K_2 \tilde{v}_0$. Then, use the iteration scheme

$$\begin{pmatrix} I & -hI & 0 \\ 0 & K_2^T L K_2 & -I \\ 0 & 0 & I \end{pmatrix} \begin{pmatrix} \tilde{q}_k \\ \tilde{v}_k \\ \tilde{p}_k \end{pmatrix} = \begin{pmatrix} I & 0 & 0 \\ 0 & 0 & 0 \\ -hK_2^T C K_2 & -hK_2^T R K_2 & I \end{pmatrix} \begin{pmatrix} \tilde{q}_{k-1} \\ \tilde{v}_{k-1} \\ \tilde{p}_{k-1} \end{pmatrix} \quad \text{for } k = 1, \dots, N \quad (3)$$

to compute $\tilde{q}_1, \dots, \tilde{q}_N, \tilde{v}_1, \dots, \tilde{v}_N$ and $\tilde{p}_1, \dots, \tilde{p}_N$.

- Midpoint rule variational integration scheme: For given $(\tilde{q}_0, \tilde{v}_0)$ compute \tilde{p}_0 via $\tilde{p}_0 = K_2^T L K_2 \tilde{v}_0$. Then, solve iteratively for $(\tilde{q}_{k+1}, \tilde{v}_{k+\frac{1}{2}}, \tilde{p}_{k+1})$, $k = 0, \dots, N - 1$ using the scheme

$$\begin{pmatrix} I & -hI & 0 \\ 0 & K_2^T L K_2 & -\frac{1}{2}I \\ \frac{1}{2}hK_2^T C K_2 & hK_2^T R K_2 & I \end{pmatrix} \begin{pmatrix} \tilde{q}_{k+1} \\ \tilde{v}_{k+\frac{1}{2}} \\ \tilde{p}_{k+1} \end{pmatrix} = \begin{pmatrix} I & 0 & 0 \\ 0 & 0 & \frac{1}{2}I \\ -\frac{1}{2}hK_2^T C K_2 & 0 & I \end{pmatrix} \begin{pmatrix} \tilde{q}_k \\ \tilde{v}_{k-\frac{1}{2}} \\ \tilde{p}_k \end{pmatrix} \quad (4)$$

for $k = 0, \dots, N - 1$.

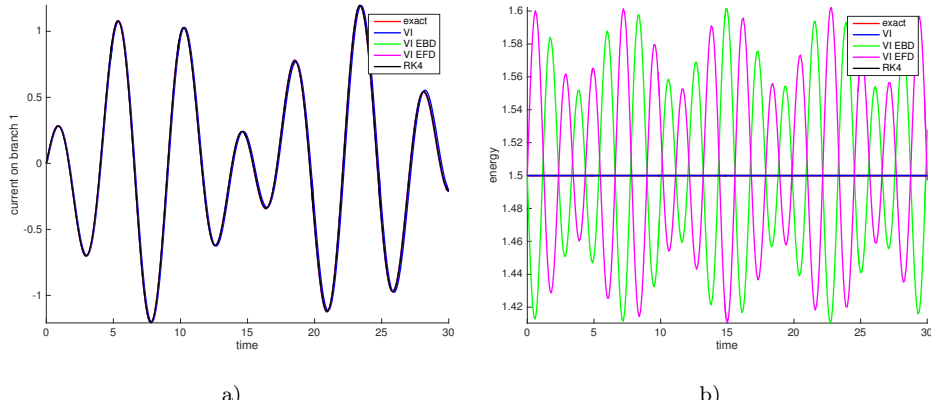


Figure 3: LC circuit (no resistors) with step size $h = 0.1$. a) The oscillating behavior of the current on the first branch is shown. b) Comparison of the exact energy behavior (exact) and the numerical solution using the three different variational integrators, midpoint rule (VI), backward Euler (VI EBD), and forward Euler (VI EFD), and a Runge-Kutta method of fourth order (RK). The energy is (qualitatively) preserved for VI, VI EBD, VI EFD, and RK.

(iv)

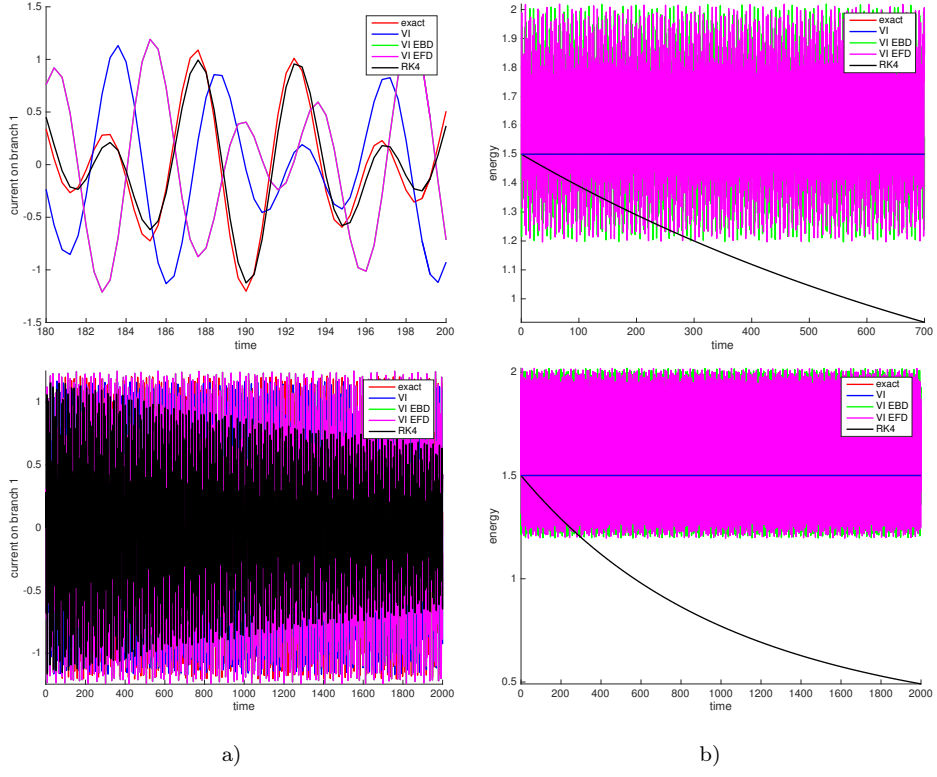


Figure 4: LC circuit (no resistors) with step size $h = 0.4$. Comparison of the exact solution (exact) and the numerical solution using the three different variational integrators, midpoint rule (VI), backward Euler (VI EBD), and forward Euler (VI EFD), and a Runge-Kutta method of fourth order (RK4). a) The use of variational integrators (VI, VI EBD, VI EFD) leads to a phase shifting in the numerical solution of the current (top). After a certain integration time, the amplitude of the current oscillations of the RK method is damped (bottom). b) The energy is (qualitatively) preserved for VI, VI EBD, and VI EFD. The use of RK4 leads to an artificial energy decay.

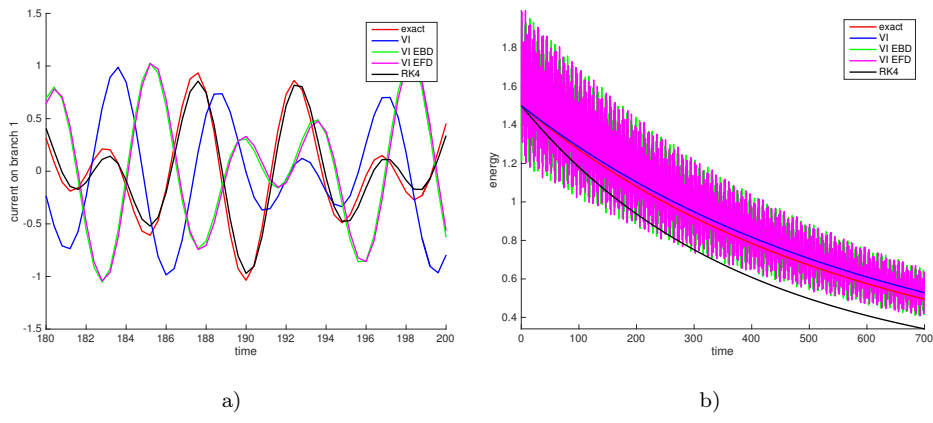


Figure 5: LCR circuit (with resistors) with step size $h = 0.4$. Comparison of the exact solution (exact) and the numerical solution using the three different variational integrators, midpoint rule (VI), backward Euler (VI EBD), and forward Euler (VI EFD), and a Runge-Kutta method of fourth order (RK4). a) The use of variational integrators (VI, VI EBD, VI EFD) leads to a phase shifting in the numerical solution of the current. b) The energy decay is much better preserved for VI, VI EBD, and VI EFD as for RK4.

5 Further reading

References

- [1] M. Arnold, A. Cardona, and O. Brüls. A Lie algebra approach to Lie group time integration of constrained systems. In P. Betsch, editor, *Structure-Preserving Integrators in Nonlinear Structural Dynamics and Flexible Multibody Dynamics*, volume 565 of *CISM Courses and Lectures*, pages 91–158. Springer International Publishing, Cham, 2016.
- [2] Olivier Brüls and Alberto Cardona. On the use of Lie group time integrators in multibody dynamics. *Journal of Computational and Nonlinear Dynamics*, 5(3):031002, 2010.
- [3] Elliot R Johnson and Todd D Murphey. Scalable variational integrators for constrained mechanical systems in generalized coordinates. *IEEE Transactions on Robotics*, 25(6):1249–1261, 2009.
- [4] Jerrold E Marsden and Matthew West. Discrete mechanics and variational integrators. *Acta Numerica 2001*, 10:357–514, 2001.
- [5] S. Ober-Blöbaum, M. Tao, M. Cheng, H. Owhadi, and J. E. Marsden. Variational integrators for electric circuits. *Journal of Computational Physics*, 242:498–530, 2013.
- [6] Sina Ober-Blöbaum, Oliver Junge, and Jerrold E Marsden. Discrete mechanics and optimal control: an analysis. *ESAIM: Control, Optimisation and Calculus of Variations*, 17(2):322–352, 2011.

Are you passionate about mobility and new technologies?
If you are, we have something in common and should get to know each other.

Our engineering excels in vehicles across the globe: We get technically perfected innovations on the road for all major car manufacturers and component suppliers. Over 6,500 members of staff work on completing exciting projects at over 30 operations with our own testing facilities – from concept to start of production, from subcompact to truck.

We can offer a wide range of career opportunities in activities such as design, simulation and testing, modeling, software development as well as developing autonomous systems. Also at our Chemnitz/Stollberg operation.

Come and join our team – we look forward to meeting you.

www.iav.com/karriere

Automotive development
thrives on innovations.
*+ people who
think ahead*



Summerschool Applied Mathematics and Mechanics (SAMM2016)



automotive
engineering

